ELSEVIER

Microporous and Mesoporous Materials 23 (1998) 277–285

MICROPOROUS AND MESOPOROUS MATERIALS

Isolation and characterization of a novel lamellar-type aluminophosphate, $AlPO_4$-L, a common precursor for $AlPO_4$ molecular sieves

N. Venkatathri, S.G. Hegde, V. Ramaswamy, S. Sivasanker *

Catalysis Division, National Chemical Laboratory, Pune 411 008, India

Received 11 December 1997; accepted 27 February 1998

Abstract

Several aluminophosphate molecular sieves ($AlPO_4$-5, $AlPO_4$-22, $AlPO_4$-16 and SAPO-35) are formed via a common lamellar aluminophosphate material ($AlPO_4$-L) during hydrothermal synthesis from a gel containing Al_2O_3, P_2O_5, SiO_2 and hexamethyleneimine (HEM) in aqueous (H_2O), or non-aqueous (ethyleneglycol, EG) media. Depending on the concentration of the template HEM, $AlPO_4$-L transforms into $AlPO_4$-5, $AlPO_4$-16 and $AlPO_4$-22, while SAPO-L transforms into SAPO-35. $AlPO_4$-L was isolated in a pure form from H_2O as well as EG media and characterized by PXRD, SEM, TG/DTA, TG/MS and FTIR spectroscopic techniques. It is a lamellar aluminophosphate, intercalating HEM and H_2O, and is thermally stable up to 250°C. $AlPO_4$-L is believed to form by the rearrangement of macroanionic $[3HEMH]^{3+}Al_3P_4O_{16}^{3-}$ sheets formed in the reaction medium.

Keywords: $AlPO_4$-L; $AlPO_4$-5; $AlPO_4$-16; $AlPOi_4$-22; Aluminophosphates; Hexamethyleneimine; Molecular sieves; SAPO-35; Synthesis

1. Introduction

Microporous and mesoporous aluminosilicates (zeolites) and aluminophosphates ($AlPO_4$) are important materials in adsorption and catalysis. As a result, new materials and new applications of known materials are being discovered [1,2]. The mechanisms of the formation of these materials, including the role of organic structure-directing agents, are also being investigated. [3] Organic templates play a complex and cooperative role in the ordering of the inorganic building blocks, as well as filling the void space and balancing the framework charge, leading to stabilization of metastable structures [4]. Meir [5] proposed that each type of structure can be built by characteristic secondary building units (SBU), which Barrer [6] suggested to be the precursors for zeolite nucleation and crystal growth. Vaughan [7] applied an extended structure approach highlighting the role of primary cations (Na^+, K^+, etc.) and secondary cations in the formation of faujasite sheets which condensed to generate EMT or faujasite structures. Davis et al. [8] proposed that hydrophobic hydration spheres of aluminosilicate species and template species should overlap (which depends on

* Corresponding author.

1387-1811/98/$19.00
PII: S1387-1811(98)00123-1

template silicate interactions) to form nuclei and lead to crystal growth. Kumar et al. [9] studied this mechanism further, and found that such overlapping can be enhanced using promoters. Recently, Lohse et al. [10] have shown that zeolite β is formed via an intermediate aluminosilicate layer structure. More recently [11], these inorganic ultrastructures were obtained over nanoscopic (<10 Å), mesoscopic (10–500 Å), microscopic (500–10 000 Å) and macroscopic (>10 000 Å) length scales using vesicular lamellar and micellar templates. Even though many such studies are available on the mechanism of formation of aluminosilicates, studies of the formation of $AlPO_4$-*n* molecular sieves are scarce. Because of the rapid product formation which occurs under hydrothermal reaction conditions, kinetic intermediates cannot be easily detected. It is commonly believed that in the early stages of $AlPO_4$-*n* formation, materials with very open structures are formed. These phases are generally of unknown structure and have not been isolated. It is believed that the gel structure transforms into a layer structure and then into a three-dimensional framework [12]. In the present paper, we report the formation of a novel lamellar-type aluminophosphate ($AlPO_4$-L) as an intermediate in the crystallization of $AlPO_4$-5, $AlPO_4$-22, $AlPO_4$-16 and SAPO-35 molecular sieves. We have isolated this intermediate phase in a pure form and characterized it using XRD, SEM, TG-DTA, TG-MS and FTIR methods. We have used hexamethyleneimine (HEM) as a template for the first time in the synthesis of $AlPO_4$-*n* molecular sieves.

2. Experimental

Synthesis of $AlPO_4$-molecular sieves was carried out using Catapal B (74.2% Al_2O_3, Vista, USA), orthophosphoric acid (H_3PO_4, 85%, s.d. fine, India), aluminium isopropoxide ([Al(i-PrO)$_3$], Aldrich, USA), fumed silica (SiO_2, Fluka), hexamethyleneimine (HEM, 98%, Aldrich) and ethylene glycol (EG, 98%, s.d. fine, India). The reactive gel composition was Al_2O_3:xP_2O_5:$ySiO_2$:zHEM:

Table 1
Reaction gel molar compositions leading to $AlPO_4$-L

Example	Gel molar composition[a]	Al source	Crystallization time	Phase	Crystallization time	Phase
1	Al_2O_3:P_2O_5:1.16HEM:45H_2O	Catapal B	24h	$AlPO_4$-5	3d	$AlPO_4$-5 + $AlPO_2$-L
			5d	$AlPO_4$-5 + $AlPO_4$-L + $AlPO_4$-22	7d	$AlPO_4$-L + $AlPO_4$-22
					9d	$AlPO_4$-22
2	Al_2O_3:P_2O_5:1.35HEM:45H_2O	Catapal B	16h	$AlPO_4$-L + $AlPO_4$-16	24h	$AlPO_4$-16
3	Al_2O_3: P_2O_5:2.32HEM:45H_2O	Catapal B	2d	$AlPO_4$-L	11d	$AlPO_4$-L
					30d	$AlPO_4$-L + $AlPO_4$-5
4	Al_2O_3:1.2P_2O_5:1.16HEM:45H_2O	Catapal B	16h	$AlPO_4$-L + $AlPO_4$-22	24h	$AlPO_4$-22
5	Al_2O_3:P_2O_5:1.16HEM:45H_2O	Al isopropoxide	16h	$AlPO_4$-L + $AlPO_4$-16	24h	$AlPO_4$-16
6	Al_2O_3:P_2O_5:2.32HEM:45H_2O	Al isopropoxide	2d	$AlPO_4$-L	11d	$AlPO_4$-L
7	Al_2O_3:1.8P_2O_5:4.5HEM:45EG	Al isopropoxide	5d	$AlPO_4$-L	15d	$AlPO_4$-5
8	Al_2O_3:1.8P_2O_5:0.3SiO_2:4.5HEM:45EG	Al isopropoxide	5d	SAPO-L	15d	SAPO-35

[a]HEM = hexamethyleneimine.

$a$$H_2O$,$b$EG, where the quantities x, y, z, a and b were varied as shown in Table 1. In a typical synthesis of $AlPO_4$-L, 7.16 g of Catapal B was mixed with 20 ml of distilled water, and 11.5 g of orthophosphoric acid was added dropwise with stirring to obtain a thick paste. A mixture of 11.64 g of hexamethyleneimine and 20 ml of water was added to this paste and stirred well. The final gel was charged into a Teflon-lined stainless-steel autoclave and placed in an oven at 473 K for eight days. The autoclave was then quenched, the product was filtered, washed with distilled water several times and dried at room temperature. Hexamethylenemine dihydrogen phosphate was prepared by mixing a 1:1 mole ratio of HEM and H_3PO_4. All the samples were characterized further by chemical analysis and XRD (Rigaku), SEM (Jeol), TG-DTA (Setaram), TG-MS (Sorbstar 200, Hungary) and FTIR (Nicolet 60SXB) spectroscopy.

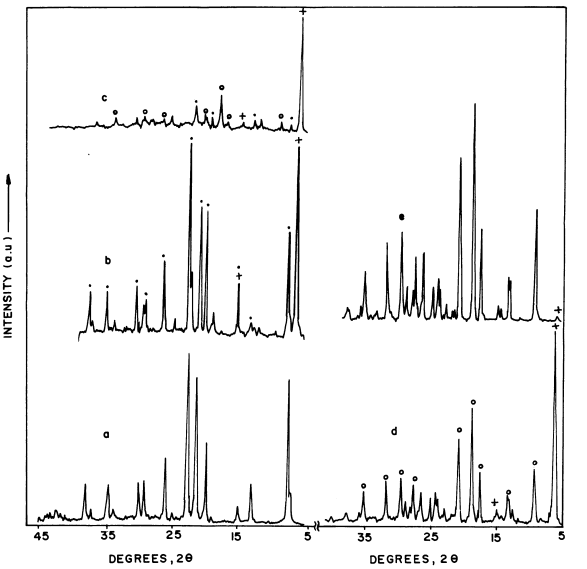

Fig. 1. X-ray diffraction patterns of (a) $AlPO_4$-5, (b) $AlPO_4$-5 + $AlPO_4$-L, (c) $AlPO_4$-5 + $AlPO_4$-L + $AlPO_4$-22, (d) $AlPO_4$-L + $AlPO_4$-22 and (e) $AlPO_4$-22.

3. Results and discussion

Hexamethyleneimine is more basic than primary, secondary and tertiary alkylamines. It has been used previously in the synthesis of MCM-22 [10], PSH-3 [11], Nonasil [12] and Dodecasil [13] molecular sieves. We have now found that HEM can be used to synthesize different $AlPO_4$ molecular sieves, depending on the synthesis conditions (Table 1). It is found that $AlPO_4$-5, $AlPO_4$-22, $AlPO_4$-16 and SAPO-35 molecular sieves can be obtained using this template. Quinuclidine is the only other template previously reported to produce all the above four molecular sieves. When Catapal B was used (Al_2O_3:1.16HEM, example 1 in Table 1) only the $AlPO_4$-5 phase nucleated, attaining 100% crystallinity in 24 h. Thereafter, the crystallinity of $AlPO_4$-5 decreased and a new phase began to grow. Continuation of crystallization revealed the following sequential transformation: $AlPO_4$-5 → $AlPO_4$-5 + $AlPO_4$-L → $AlPO_4$-5 + $AlPO_4$-L + $AlPO_4$-22 → $AlPO_4$-L + $AlPO_4$-22 → $AlPO_4$-22. The XRD patterns of the pure $AlPO_4$ phases and the mixtures are presented in Fig. 1. This transformation is also seen in the SEM pictures (Fig. 2). The pure form of the new intermediate phase $AlPO_4$-L was, however, not obtained in this gel composition. When the concentration of HEM was increased to 1.35 moles per mole of Al_2O_3 (example 2), within 15 h, $AlPO_4$-L + $AlPO_4$-16 appeared, which transformed into pure $AlPO_4$-16 within 24 h. On increasing the concentration further to 2.32 moles (example 3), within 48 h, the pure $AlPO_4$-L phase appeared and grew fully, remaining stable even up to 20 days. A similar trend appeared when 1.2 moles P_2O_5 were added per mole of Al_2O_3: $AlPO_4$-L + $AlPO_4$-22 formed in 15 h, and transformed into $AlPO_4$-22 in 24 h (example 4). When aluminium isopropoxide [Al(i-OPr)$_3$] was used (example 5), keeping all other constituents the same as in example 1, $AlPO_4$-L + $AlPO_4$-16 appeared in 15 h, which led to pure $AlPO_4$-16. However, aluminium isopropoxide gave pure $AlPO_4$-L if the composition of example 3 was used (example 6). Examples 7 and 8 were synthesised in ethylene glycol. The reactant compositions were comparable to those recently reported [13,14] for some $AlPO_4$ materials prepared in non-aqueous media. $AlPO_4$-L crystallized within three days in EG medium (example 7), transforming into $AlPO_4$-5 in ten days, which was

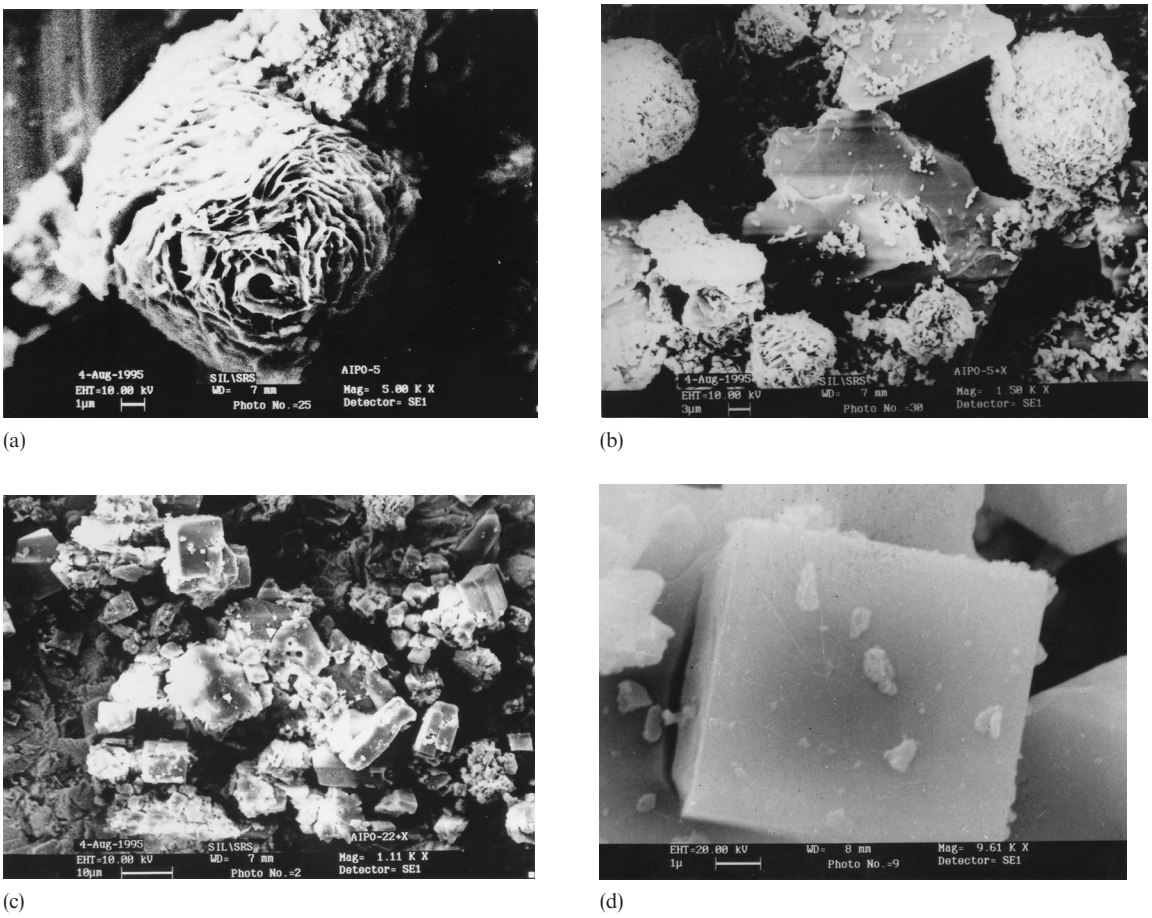

Fig. 2. SEM photographs (aqueous medium) of (a) $AlPO_4$-5, (b) $AlPO_4$-5 + $AlPO_4$-L, (c) $AlPO_4$-L + $AlPO_4$-22 and (d) $AlPO_4$-22.

stable in this medium for a long time (at least 90 days). The transformation of $AlPO_4$-L into $AlPO_4$-5 can be seen clearly in the SEM pictures presented in Fig. 3. Introducing silica (0.3 M) into this composition (example 8) led to SAPO-35 through SAPO-L instead of $AlPO_4$-5 [15]. SAPO-35 was also found to be stable in this reaction medium.

The fact that all the above structure types were obtained from similar reaction mixtures suggests the existence of a close structural relationship between these phases, possibly linked through a common precursor $AlPO_4$-L phase. Richardson et al. [16] and Keller et al. [17] have postulated that crankshaft-type chains formed by an alternating connection of Al^{3+} and P^{5+} through bridging O^{2-} can be interconnected to form double-crankshaft structures, which can be viewed as the building blocks for $AlPO_4$-*n* molecular sieves such as $AlPO_4$-5, $AlPO_4$-21, $AlPO_4$-C and $AlPO_4$-11. Li et al. [18] considered the triple crankshaft formed by the interconnection of single crankshafts as building blocks of VPI-5, $AlPO_4$-H3 and tridymite. However, it was Oliver et al. [19] who demonstrated experimentally the formation of such crankshaft structures. They showed that when pseudoboehmite reacted with H_3PO_4 in the presence of triethylamine in a non-aqueous medium, primarily anionic $[AlP_2O_8H_2]^-$ chains were formed which hydrolysed to form Al–O–P chains of different configurations. These chains formed double- or triple-crankshaft chains of different

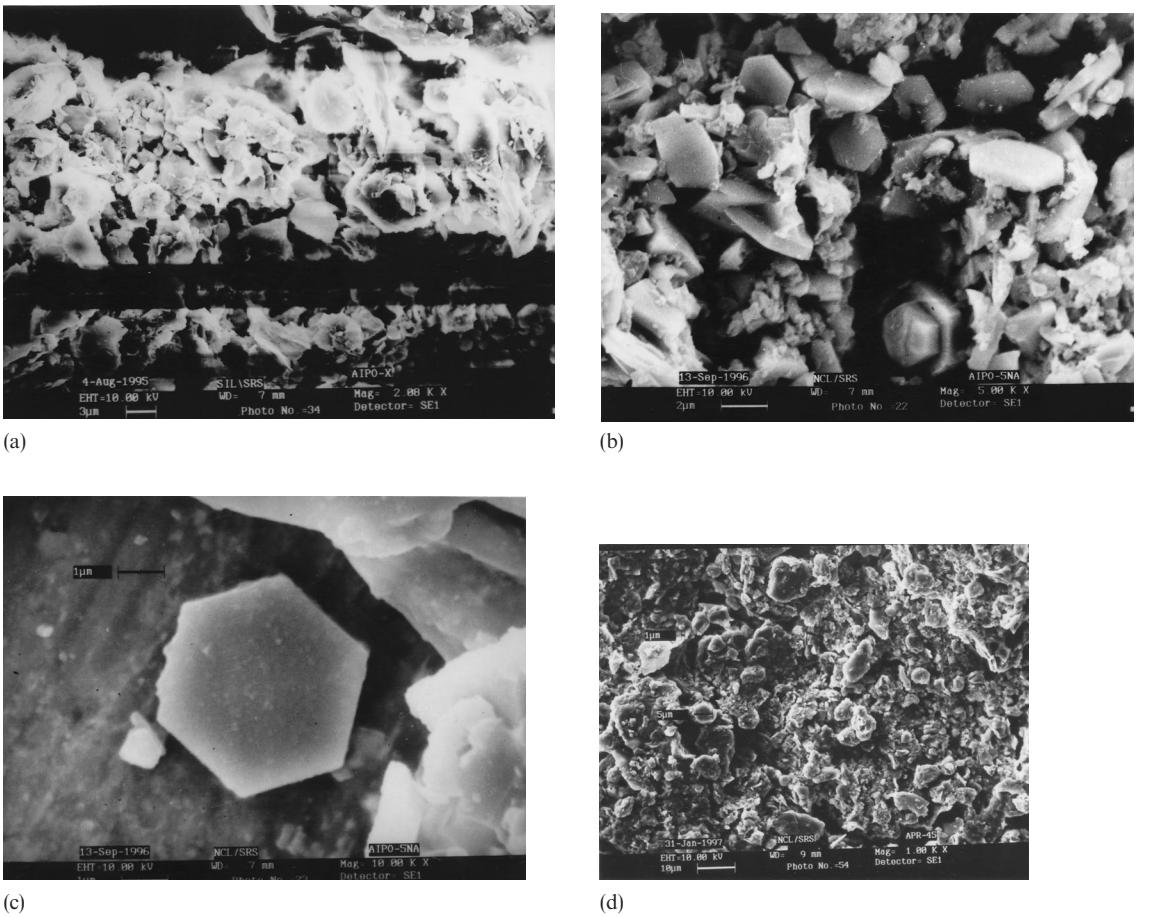

(a) (b)

(c) (d)

Fig. 3. SEM photographs (non-aqueous medium) of (a) $AlPO_4$-L, (b) $AlPO_4$-L + $AlPO_4$-5, (c) $AlPO_4$-5 and (d) $AlPO_4$-L (aqueous medium).

configurations, the precursors of $AlPO_4$-*n* materials. Even though they characterized structurally them using XRD methods, no pure phases were obtained.

Fig. 4 presents the XRD patterns of the $AlPO_4$-L and $AlPO_4$-16 obtained from the aqueous medium, and SAPO-L and SAPO-35 obtained from the non-aqueous medium. Fig. 4 shows that the $AlPO_4$-L obtained in this study was a highly crystalline material, and also indicates the absence of any hexamethyleneimine dihydrogen phosphate impurity. There were three sharp diffraction lines at *d* values of 14.2, 7.1 and 4.8 Å, indicating the product to be a short-range ordered lamellar-type aluminophosphate. It seems that when pseudo-boehmite was reacted with H_3PO_4 in the presence of the HEM template, $[AlP_2O_8H_2]^-[HEMH]^+$ chains were produced which hydrolyzed to form –Al–O–P– crankshaft-type chains, similar to those suggested for triethylamine by Oliver et al. [19]. Double- or triple-crankshaft chains were formed by condensation of these chains to produce the intermediate $AlPO_4$-L lamellar structure. Being a very open structure, it hydrolyses further into secondary chain-building units which reassemble to form more stable condensed $AlPO_4$-*n* molecular sieves.

The lamellar $AlPO_4$-L material (Fig. 4) was stable only up to 250°C. Heating to higher temperatures to remove the occluded template led to an

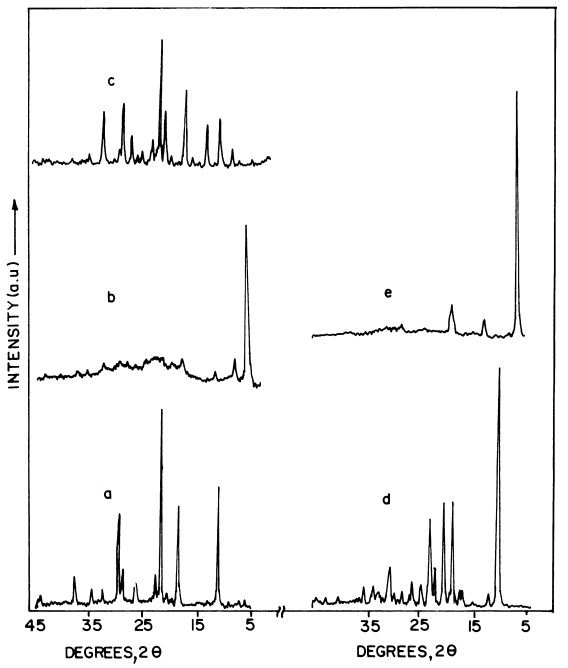

Fig. 4. X-ray diffraction patterns of (a) $AlPO_4$-16, (b) SAPO-L, (c) SAPO-35, (d) HEM dihydrogen phosphate and (e) $AlPO_4$-L.

amorphous material. However, when Si was introduced, SAPO-L was stable up to 350°C. Elemental analysis of $AlPO_4$-L showed the chemical composition to be Al_2O_3:1.3P_2O_5:2HEM, similar to the $[Al_3P_4O_{16}]^{3-}3[HEMH]^+$ chains suggested by Oliver et al. [19].

The TG-DTA curves (Fig. 5) for $AlPO_4$-L and $AlPO_4$-5 revealed the presence of three stages of weight loss, as summarized in Table 2. The large initial endothermic weight loss of about 18% in the range 25–300°C reveals the presence of large amounts of water molecules occluded in the layers

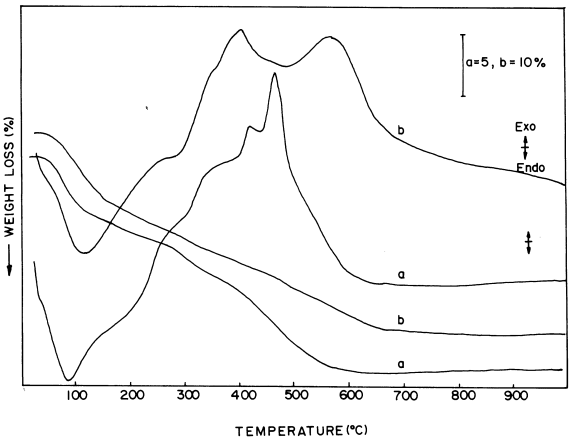

Fig. 5. TG-DTA patterns of (a) $AlPO_4$-5 and (b) $AlPO_4$-L.

along with the template. The other two exothermic peaks, at around 415 and 567°C for $AlPO_4$-L and at 380 and 474°C for $AlPO_4$-5, are due to the oxidative decomposition of the occluded template. The slightly higher temperature of combustion of the template in $AlPO_4$-L than in $AlPO_4$-5 may be due to the collapse of the lamellar structure above 250°C, trapping the fragmentation products of the template in the former materials. TG-MS showed (Fig. 6) that HEM decomposed in a He atmosphere into NH_3, $CH_2{=}CH_2$ and CH_4, leaving a carbonaceous residue behind. TG-MS also revealed a higher temperature of desorption of the fragmentation products from $AlPO_4$-L as compared to $AlPO_4$-5.

FTIR spectra of $AlPO_4$-L and $AlPO_4$-5 in the framework vibration region are presented in Fig. 7. $AlPO_4$-L showed bands at 1150(w), 1030(vs), 904(sh), 760(w), 670(s), 606(vw), 547(m), 584(m) and 430(vw) cm^{-1}. The assign-

Table 2
TG/DTA analysis of $AlPO_4$-L and $AlPO_4$-5

Structure	Weight loss (temperature range, °C)			Peak positions (°C)		
	Stage I	Stage II	Stage III	Stage I	Stage II	Stage III
$AlPO_4$-L	17% (25–285)	8% (285–489)	8% (489–526)	111	415	567
$AlPO_4$-5	6.4% (25–211)	5% (211–404)	6.5% (404–715)	85	360	474

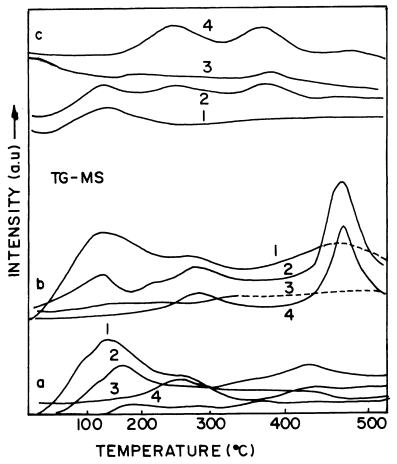

Fig. 6. TG-MS patterns of (a) $AlPO_4$-5, (b) $AlPO_4$-22 and (c) $AlPO_4$-L. (1) H_2O, (2) NH_3, (3) $CH_2{=}CH_2$ and (4) CH_4.

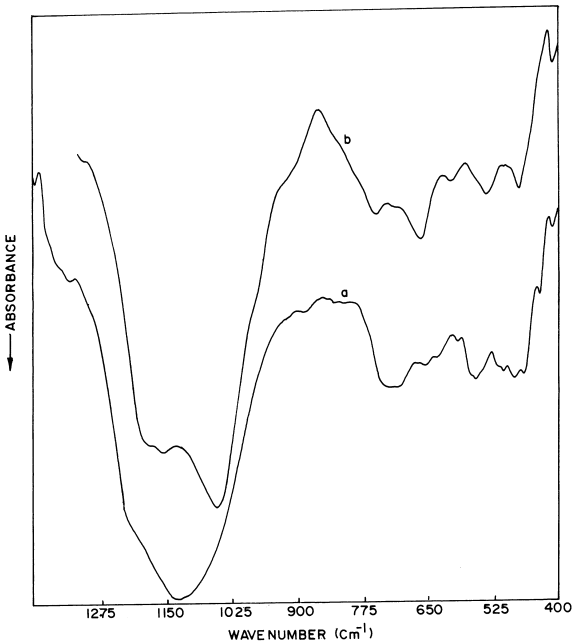

Fig. 7. Diffuse reflectance FTIR spectra of (a) $AlPO_4$-5 and (b) $AlPO_4$-L.

ments for these bands, based on literature data, are given in Table 3 in comparison with those of $AlPO_4$-5. All the band positions of $AlPO_4$-L were shifted to lower wave numbers as compared to $AlPO_4$-5.

The transformation of the reaction gel into different $AlPO_4$-*n* molecular sieves through a layer-structure $AlPO_4$-L is shown schematically in Fig. 8. The formation of $[AlP_2O_8H_2]^-$ chains and $[Al_3P_4O_{16}]^{3-}$ layer chains by the reaction of Al_2O_3, H_3PO_4 and template has been proposed by Oliver et al. [19]. When these charged layer chains are assembled, occluding $HEMH^+$ species between layers, we obtain the stable structure of $AlPO_4$-L. The distance between these –Al–O–P– layers in the $AlPO_4$-L structure shown in Fig. 8 was calculated by a molecular modelling method using the package Insight II, supplied by Molecular Simulation Inc., USA. The template and the water molecules were built as molecular models. The packing of the molecules was performed by a molecular fitting technique. It was found that the inter-layer distance is $\sim$14.0 Å, with the template and water molecules clatherated between the layers. This distance is in fair agreement with the distance (14.2 Å) obtained from the XRD results. Thermal analysis data have revealed the presence of two types of occluded HEM molecules, i.e. weakly held neutral HEM and strongly held protonated HEM ($HEMH^+$), between the aluminophosphate sheets. Weakly bound neutral HEM molecules desorbed below 250°C, while the strongly bound $HEMH^+$ species desorbed after decomposition at higher temperatures. Depending upon the concentration of HEM, P_2O_5 and the medium of synthesis (aqueous or non-aqueous),

Table 3
FTIR bands for $AlPO_4$-L and $AlPO_4$-5 synthesized from hexamethyleneimine template

Sample	Asymmetric stretching		Symmetric stretching		Double rings	T–O–T bending	Pore opening
	Internal	External	Internal	External			
$AlPO_4$-L	1150(w)	1030(vs), 904(sh)	760(w)	670(s)	606(vw)	547(m)	430(vw)
$AlPO_4$-5	1215(w)	1130(vs)	725(m)	700(m)	645(vw)	565(m)	425(vw)

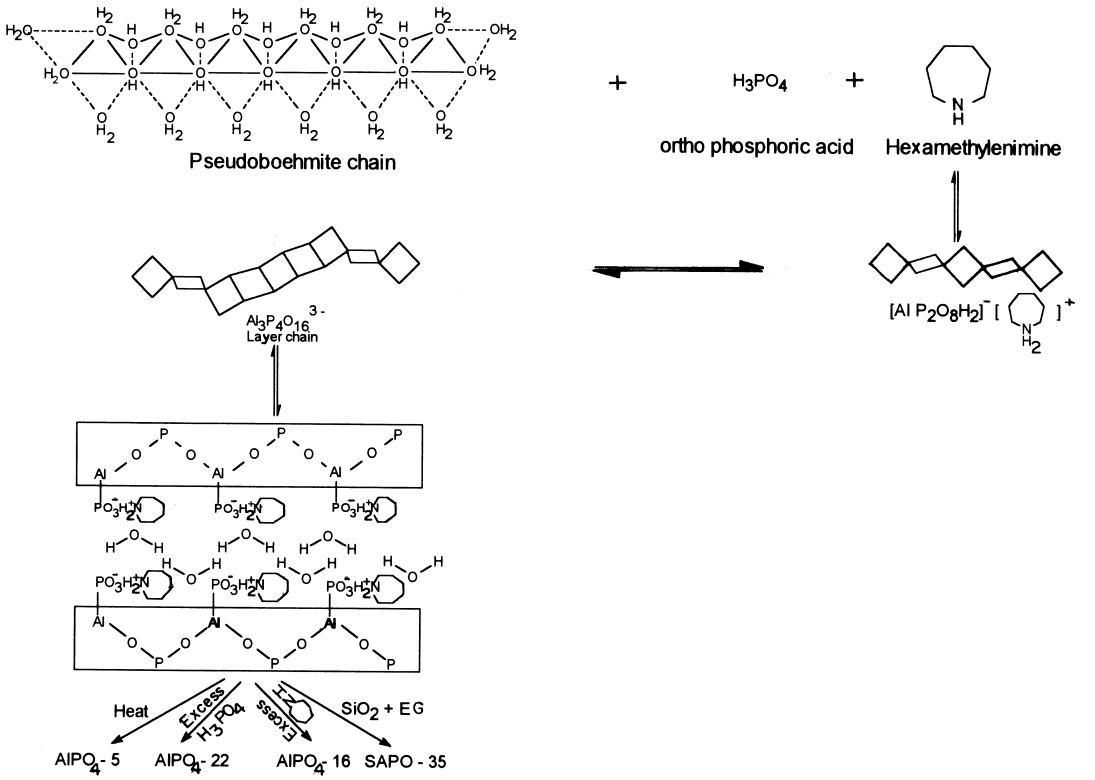

Fig. 8. A schematic route for the formation of $AlPO_4$ molecular sieves from the layer material ($AlPO_4$-L).

the $AlPO_4$-L layer structure transformed into $AlPO_4$-5, $AlPO_4$-16, $AlPO_4$-22 and SAPO-35.

4. Conclusions

The present study demonstrates the importance of a layer-structured material ($AlPO_4$-L) as the common intermedidate in the formation of $AlPO_4$-5, $AlPO_4$-16, $AlPO_4$-22 and SAPO-35 molecular sieves. The layer-structured $AlPO_4$-L has been isolated for the first time and characterized by PXRD, SEM, TG-DTA, TG-MS and FTIR spectroscopic methods. During the hydrothermal synthesis, $AlPO_4$-L was obtained in a pure form only at a high concentration of the HEM template (>2.35 moles per mole of Al_2O_3 mole). Although $AlPO_4$-L was stable only up to 250°C, SAPO-L was stable up to 350°C.

Acknowledgement

We thank Dr. R. Vetrivel for carrying out the molecular modelling analysis.

References

[1] D. Zhao, Z. Luan, L. Kevan, Chem. Commun. (1997) 1009.
[2] P.A. Barret, R.H. Jones, J.M. Thomas, G. Sanker, I.J. Shannon, C.R.A. Catlow, Chem. Commun. (1996) 2001.
[3] M.E. Davis, S.I. Zones, in: M.L. Occelli, H. Kessler (Eds.), Synthesis of Porous Materials, Marcel Dekker Inc., New York, 1996, p. 1.
[4] E.J.P. Faijen, J.A. Martens, P.A. Jacobs, Stud. Surf. Sci. Catal. 84 (1994) 3.
[5] W.M. Meier, in: Molecular Sieves, Society of the Chemical Industry, London, 1968, p. 10.

[6] R.M. Barrer, in: Hydrothermal Chemistry of Zeolites, Academic Press, London, 1982, p. 105.
[7] D.E.W. Vaughan, in: G. Ohlmann, H. Pfeifer, R. Fricke (Eds.), Catalysis and Adsorption by Zeolites, Elsevier, Amsterdam, 1991, p. 275.
[8] M.E. Davis, in: L. Bonneviot, S. Kaliaguine (Eds.), Zeolites: A Refined Tool for Designing Catalytic Sites, Elsevier, Amsterdam, 1995, p. 35.
[9] R. Kumar, A. Bhoumick, R.K. Ahedi, S. Ganapathy, Nature 381 (1996) 298.
[10] U. Lohse, B. Altrichter, R. Fricke, W. Pilz, E. Schreier, C. Garkisch, K. Janke, J. Chem. Soc., Faraday Trans. 93 (1997) 505.
[11] G.A. Ozin, S. Oliver, Adv. Mater. 7 (1995) 943.
[12] D.J.E. Mueller, J. Richter-Mendau, in: M.L. Ocelli, H.E. Robson, (Eds.), Synthesis of Microporous Materials, Nelson Canada, Scarborough, 1992, p. 1.
[13] Q. Gao, S. Li, R. Xu, J. Chem. Soc., Chem. Commun. (1994) 1465.
[14] H. Qisbeng, X. Ruren, J. Chem. Soc., Chem. Commun. (1990) 783.
[15] N. Venkatathri, S.G. Hegde, P.R. Rajamohanan, S. Sivasanker, J. Chem. Soc., Faraday Trans. 93 (1997) 3411.
[16] J.W. Richardson, J.V. Smith, J.J. Pluth, J. Phys. Chem. 93 (1989) 8212.
[17] E.B. Keller, W.M. Meier, R.M. Kirchner, Solid State Ionics 43 (1990) 93.
[18] H. Li, M.E. Davis, J.B. Higgins, R.M. Dessau, J. Chem. Soc., Chem. Commun. (1993) 403.
[19] S. Oliver, A. Kuperman, A. Lough, G.A. Ozin, J.M. Garces, M.M. Olken, P. Rudolf, Stud. Surf. Sci. Catal. 84 (1994) 219.